ARTICLE

Identification of Somatic Chromosomal Abnormalities in Hypothalamic Hamartoma Tissue at the *GLI3* Locus

David W. Craig,[1,4,*] Abraham Itty,[1,4] Corrie Panganiban,[1] Szabolcs Szelinger,[1] Michael C. Kruer,[2] Aswin Sekar,[1] David Reiman,[1] Vinodh Narayanan,[3] Dietrich A. Stephan,[1] and John F. Kerrigan[3]

Hypothalamic hamartomas (HH) are rare, benign congenital tumors associated with intractable epilepsy. Most cases are sporadic and nonsyndromic. Approximately 5% of HH cases are associated with Pallister-Hall syndrome (PHS), which is caused by haploinsufficiency of *GLI3*. We have investigated the possibility that HH pathogenesis in sporadic cases is due to a somatic (tumor-only) mutation in *GLI3*. We isolated genomic DNA from peripheral blood and surgically resected HH tissue in 55 patients with sporadic HH and intractable epilepsy. A genome-wide screen for loss of heterozygosity (LOH) and chromosomal abnormalities was performed with parallel analysis of blood and HH tissue with Affymetrix 10K SNP microarrays. Additionally, resequencing and fine mapping with SNP genotyping were completed for the *GLI3* gene with comparisons between peripheral blood and HH tissue pairs. By analyzing chromosomal copy-number data for paired samples on the Affymetrix 10K array, we identified a somatic chromosomal abnormality on chromosome 7p in one HH tissue sample. Resequencing of *GLI3* did not identify causative germline mutations but did identify LOH within the *GLI3* gene in the HH tissue samples of three patients. Further genotyping of 28 SNPs within and surrounding *GLI3* identified five additional patients exhibiting LOH. Together, these data provide evidence that the development of chromosomal abnormalities within *GLI3* is associated with the pathogenesis of HH lesions in sporadic, nonsyndromic patients with HH and intractable epilepsy. Chromosomal abnormalities including the *GLI3* locus were seen in 8 of 55 (15%) of the resected HH tissue samples. These somatic mutations appear to be highly variable.

Introduction

Hypothalamic hamartomas (HH [MIM 241800]) are uncommon, benign congenital tumors, associated with refractory epilepsy, and occur in approximately one in 200,000 children and adolescents.[1] Symptoms resulting from HH include gelastic seizures, cognitive deficits, and behavioral abnormalities.[2] This phenotype is highly associated with the intrahypothalamic anatomic type of HH, whereas the parahypothalamic type usually results in central precocious puberty only.[3–5] A progressive clinical course with worsening of seizures, cognition, and behavior is seen in at least 50% of cases.[6–8] Those with onset of epileptic seizures during infancy appear to be at greatest risk for this deteriorating natural history. Approximately 40% of patients with the intrahypothalamic type of HH also have central precocious puberty.[9]

Most HH patients develop the disease on a sporadic, nonfamilial basis. However, HH is described in association with a number of different dysmorphic syndromes.[10] Of these, by far the most common is Pallister-Hall syndrome (PHS [MIM 146510]), which accounts for approximately 5% of all HH patients with epilepsy.[8] Clinical features of PHS include HH, central or postaxial polydactyly, imperforate anus, and bifid epiglottis.[11] Affected pedigrees indicate autosomal-dominant inheritance with variable expressivity, although most cases are sporadic and represent new mutations.[12]

Linkage analysis of large PHS pedigrees suggested a susceptibility locus at 7p13.[13] Utilizing a candidate gene approach, the same group reported that two affected families had frameshift (loss-of-function) mutations in *GLI3* (MIM 165240), a zinc-finger transcription factor within the sonic hedgehog intracellular signaling pathway.[14]

Although HH occurs in PHS as a result of a genomic mutation, we have investigated the possibility that HH in sporadic, nonsyndromic cases results from a somatic (tumor-only) chromosomal abnormality or *GLI3* mutation. We have completed a genome-wide screen for loss of heterozygosity (LOH) with comparison of single-nucleotide polymorphism (SNP) microarrays of DNA derived from blood and resected HH tissue from sporadic, nonsyndromic patients. Additionally, we have resequenced the *GLI3* coding sequences and performed fine mapping with SNPs neighboring *GLI3*, comparing DNA derived from blood and HH tissue in sporadic HH cases. Our findings identify somatic *GLI3* mutations in sporadic HH cases, suggesting a role in the etiology of HH lesions.

Material and Methods

Clinical Profile of Study Subjects

Blood and HH tissue samples for DNA studies were obtained from 55 sporadic, nonsyndromic HH patients undergoing surgical resection of HH for refractory epilepsy at our institution between February 2003 and October 2005. Fifteen patients were female (27%), and 40 were male (73%). The mean age at time of evaluation and surgical treatment was 13.8 years (median 11.8 years, range 0.7 to 39.3 years). Intractable epilepsy (failure of at least

[1]The Translational Genomics Research Institute, Neurogenomics Division, Phoenix, AZ 85004, USA; [2]Department of Pediatrics, Phoenix Children's Hospital, Phoenix, AZ 85016, USA; [3]Division of Pediatric Neurology and Comprehensive Epilepsy Program, Barrow Neurological Institute and Children's Health Center, St. Joseph's Hospital and Medical Center, Phoenix, AZ 85013, USA
[4]These authors contributed equally to this work.
*Correspondence: dcraig@tgen.org
DOI 10.1016/j.ajhg.2007.10.006.

three antiepilepsy drugs [AEDs]) was present in 100% of patients. The mean age at first onset of seizures was 1.1 years (range <0.1 to 7.0 years). However, 28 (51%) patients had onset of gelastic seizures before 1 month of age by retrospective history. All patients (100%) had gelastic seizures at some time during the clinical course, although 44 (80%) had developed at least one additional seizure type by the time of surgery (mean 2.8 seizure types per patient in those with multiple seizure types). Seizure frequency was at least 1 per day in 50 patients (91%) and at least 1 per week in the remaining five patients (9%).

Developmental retardation (IQ or developmental quotient less than 70) was present in 35 patients (64%). A prior history of central precocious puberty had occurred in 18 patients (33%). Anatomic type of the HH lesion, according to the classification system proposed by Delalande and Fohlen,[15] was type I in four (7%), type II in 35 (64%), type III in 11 (20%), and type IV in five (9%). The mean HH lesion volume was 3.25 cm^3 (median 1.25 cm^3, range 0.1 to 28.3 cm^3). Two patients (3%) had magnetic resonance (MR) imaging abnormalities in addition to the HH lesion, with periventricular nodular heterotopias in both.

Sample Collection

Genomic DNA was isolated from fresh whole blood samples, obtained prior to surgery. Surgically resected HH tissue specimens were immediately immersed in RNAlater (Applied Biosystems, Foster City, CA) and frozen at −80°C. At the time of study, genomic DNA was isolated with the Gentra Puregene DNA Purification Kit for whole tissue (Gentra Systems, Minneapolis, MN) according to the manufacturer's protocol. DNA concentration was determined with a GeneQuant spectrophotometer (Biochrom, Cambridge, UK).

Whole-Genome SNP Microarrays

SNP genotyping was performed with the GeneChip Mapping 10K Array and Assay Kit (Affymetrix, Santa Clara, CA).[16] All incubations were done with a Tetrad thermal cycler (MJ Research, Cambridge, MA). Internal positive and negative controls were performed in parallel with the supplied genomic DNA (Affymetrix). Two-hundred fifty nanograms of double-stranded genomic DNA was digested with XbaI (New England Biolabs, Ipswitch, MA) for 2 hr at 37°C, and heat inactivation for 20 min at 70°C followed. Digested DNA was then incubated with a 0.25 M *Xba* adaptor (Affymetrix) and DNA ligase (New England Biolabs) in standard ligation buffer (New England Biolabs) for 2 hr at 16°C, and heat inactivation for 20 min at 70°C followed. Ligated products were amplified in quadruplicate with 0.5 M the supplied generic primer XbaI (Affymetrix) in PCR Buffer II (Applied Biosystems) with 2.5 mM $MgCl_2$, 2.5 mM deoxynucleosides (dNTPs), and 10 units of AmpliTaq Gold polymerase (Applied Biosystems) under the following polymerase chain reaction (PCR) conditions: 95°C for 5 min, then 35 cycles (95°C for 20 s, 59°C for 15 s, and 72°C for 15 s) and a final extension at 72°C for 7 min. Fragments in the 250 to 1000 basepair size range are preferentially amplified under these conditions. PCR products were purified with the QIAquick PCR purification kit (QIAGEN, Valencia, CA) according to the manufacturer's recommendations, with the exception of the elution procedure. DNA from each of four PCR replicate samples was bound to separate columns and washed. The eluant collected from column one was used for the elution of the remaining three columns in series. The final purified product is the combination of four purified PCR product samples. Eighteen to twenty micrograms of purified PCR products were fragmented with 0.24 units of the supplied GeneChip Fragmentation Reagent (Affymetrix) for 30 min at 37°C, and a heat inactivation for 15 min at 95°C followed. Samples were then labeled with 102 units of terminal deoxytransferase (Affymetrix) and 0.143 mM of supplied GeneChip DNA Labeling Reagent in TdT buffer (Affymetrix) for 2 hr at 37°C and then 15 min at 95°C. After the end labeling, the fragments were hybridized to a GeneChip Human Mapping 10K Array for 16–18 hr at 48°C while rotating at 60 rpm. Microarrays were washed with the Fluidics Station 450 (Affymetrix) in 0.6× sodium chloride, sodium phosphate, and ethylenediaminetetraacetic acid (SSPE), and a three-step staining protocol followed. We incubated the arrays first with 10 μg/ml streptavidin (Pierce Biotechnology, Rockford, IL), washed the arrays with 6× SSPE and incubated with 5 μg/ml biotinylated antistreptavidin (Vector Laboratories, Burlingame, CA) and 10 μg/ml streptavidin-phycoerythrin conjugate (Molecular Probes, Invitrogen, Carlsbad, CA), and finally washed the arrays with 6× SSPE, per the manufacturer's recommended times. Microarrays were scanned with the GeneChip Scanner 3000 according to the manufacturer's protocol (Affymetrix). Data acquisition was performed with the GeneChip GCOS software (Affymetrix). Prior to publication, we did explore the utility of other higher density arrays for fine mapping the *GLI3* locus with sample 2030 and 450S DUO arrays (Illumina, San Diego) by using 150 ng of DNA, otherwise following manufacture recommendations. We did not attempt additional samples on this or other platforms because of limitations in available nonamplified DNA. Call rates of 98.1% and 99.1% were obtained for tissue and blood, respectively, with a reduced quantity of starting genomic DNA (150 ng versus 750 ng). Unfortunately, no informative heterozygote SNPs were found, and the region could not be further mapped. Investigation of probe intensity at the homozygote SNPs did not show evidence for a change in copy number, suggesting that tandem loss of an allele and duplication resulting in no net copy-number change is a possible mechanism for the LOH observed in the Sanger resequencing and two methods of SNP genotyping with this sample. The 450S data does further rule out contamination, degradation, or other experimental artifacts for this sample because LOH was not observed elsewhere, consistent with the Affymetrix 10K results.

GLI3 Resequencing

GLI3 encompasses approximately 250 kb across 15 exons on chromosome 7p13. *GLI3* was amplified by PCR with 2.5 mM dNTPs, 2 units of AmpliTaq Gold polymerase (Applied Biosystems), 3 mM $MgCl_2$, 5% dimethyl sulfoxide (DMSO), 1× PCR Buffer, an annealing temperature of 51.8°C, and an extension time of 1 min, and was cycled 35 times with a Tetrad thermal cycler (MJ Research, Cambridge, MA) (see Table 1). Amplified *GLI3* product was purified after thermocycling with the AmPure PCR purification kit (Agencourt Biosciences, Beverly, MA), resulting in the removal of unincorporated dNTPs, primers, and salts. PCR products were eluted in 30 μl distilled H_2O. Both strands of each PCR product were sequenced as follows: Sequencing reactions were performed with 3 μl (approximately 25 ng) of purified PCR product in a 6 μl reaction containing 0.33 μl BigDye Terminator v3.1 premix (Applied Biosystems), 3.2 pmol of either M13 forward (5′-TGTAAAACGAC GGCCAGT-3′) or M13 reverse (5′-CAGGAAACAGCTATGACC-3′) primer, and 1.03 μl 5× BigDye sequencing buffer. Cycle sequencing was performed for 35 cycles following the manufacturer's recommendations on GeneAmp 9700 PCR machines (Applied Biosystems). Sequencing reactions were purified with CleanSEQ

Table 1. Primer Sets for Amplification

Primer Sequence	Primer Name	Primer Sequence	Primer Name
5′-TGGCCAGACCTAAGAAATGC-3′	Exon 1a Forward	5′-TTGATTCCACATGGAAAAGTTG-3′	Exon 1a Reverse
5′-TGTGGAATCAAGAGCGTGTT-3′	Exon 1b Forward	5′-TTTTAAAGCCACGTCTGCAA-3′	Exon 1b Reverse
5′-GCAGACGTGGCTTTAAAAAGTA-3′	Exon 1c Forward	5′-CAAAAGTCCACTTCACCTGTCA-3′	Exon 1c Reverse
5′-TTTGGAAAGTTGATGGCTCTG-3′	Exon 2 Forward	5′-GCAAACGCTCAATTCACAAG-3′	Exon 2 Reverse
5′-GGGAGAGGGATATCGAGAATG-3′	Exon 3 Forward	5′-GGAAAGTGGAAAGAAAATTACACC-3′	Exon 3 Reverse
5′-TTGCTTTGTGAATCGGAATG-3′	Exon 4 Forward	5′-TTCAGTGAACCCACGAACAG-3′	Exon 4 Reverse
5′-AGAGACAGCCTCTGCCTGTG-3′	Exon 5 Forward	5′-GGCACATGGGAAACACTCAC-3′	Exon 5 Reverse
5′-AATTGCTGATGTGGGTTGTG-3′	Exon 6 Forward	5′-TTTGCCATTTCCCAAGACTC-3′	Exon 6 Reverse
5′-TCTTCCACGTAGGCAAGTAGC-3′	Exon 7 Forward	5′-TTCTTCCTCATAGGCAGTTGG-3′	Exon 7 Reverse
5′-GCTGCAGATCTTGTGTACTTGTC-3′	Exon 8 Forward	5′-GAGGCTGTGAGAACACAGAGG-3′	Exon 8 Reverse
5′-GCCAAATAAGACCGCTTGTC-3′	Exon 9 Forward	5′-GGAACTGCCGTGAAAAAGAC-3′	Exon 9 Reverse
5′-TTGTCTTCCCTCCTGTTGTG-3′	Exon 10 Forward	5′-CAATGCGGCTCCTAAGAAAC-3′	Exon 10 Reverse
5′-TGGGGTATTTTCTGCATTTTC-3′	Exon 11 Forward	5′-ACCGAGGCATTTATCACCAG-3′	Exon 11 Reverse
5′-CAACTTGGAGGGCGTGTTAG-3′	Exon 12 Forward	5′-TCCCACCTAGGAAGCTCAAG-3′	Exon 12 Reverse
5′-CCTCAAAGCCTTGTGAAAGTG-3′	Exon 13 Forward	5′-CCCTCTATGCACCCTACCTG-3′	Exon 13 Reverse
5′-GAGCTCTCATTATTGGC-3′	Exon 14 Forward	5′-ACTGGTGGAGAAACTAGC-3′	Exon 14 Reverse
5′-TTGCTCATGCCTGGTGTAAG-3′	Exon 15a Forward	5′-TCTTCAGGCTCATCCTCTCC-3′	Exon 15a Reverse
5′-ACTCCTACGACCCCATCTCC-3′	Exon 15b Forward	5′-ATCGTTCAGGTTGGCATCAG-3′	Exon 15b Reverse
5′-CAGTCCCGAAACTTCCACTC-3′	Exon 15c Forward	5′-ACCGTAGGGGTTGCTGTTC-3′	Exon 15c Reverse
5′-CTCCTCCAAGCTCAAGTGTG-3′	Exon 15d Forward	5′-CTGGCCCTTGGTAGATGTTG-3′	Exon 15d Reverse
5′-GGTAGCGCCAAATGAGTCAG-3′	Exon 15e Forward	5′-CGTGTCTTGCTGACTGAAGC-3′	Exon 15e Reverse
5′-GCAGTCAGGACAGCTCAGTG-3′	Exon 15f Forward	5′-GAACTCATGTCCCCGATAGC-3′	Exon 15f Reverse
5′-GACCACTCCAGCCTGATGTC-3′	Exon 15g Forward	5′-GTTAGGTGAGATGAGATTGC-3′	Exon 15g Reverse

M13 tails were added for sequencing of *GLI3*.

(Agencourt Biosciences) for the removal of unincorporated dye terminators and analyzed on 3730xl DNA analyzers (Applied Biosystems). Mutations were detected by analysis of sequences traces with Mutation Surveyor software (Soft Genetics, State College, PA).

Fine Mapping SNP Genotyping

In order to identify the extent and boundaries of LOH, we used a melting temperature (Tm)-shift SNP genotyping method, where GC tails of different lengths were attached onto the 5′ end of allele-specific primers.[17] On the basis of the melting temperature of the PCR product, SNP alleles can be distinguished, and genotypes can be assigned on the basis of the melting-curve data. Primers were designed on the basis of the methodology used by Wang et al.[17] In brief, for every SNP analyzed, we designed two forward allele-specific primers, with the 3′ end of the primer representing one of the SNP base pairs along with one common reverse primer. A 14 base pair GC clamp (5′-GCGGGCAGGGCGGC-3′) was attached to the allele-specific primer that had the higher Tm base (C or G), and a 6 base pair GC clamp (5′-GCGGGC-3′) was attached to the primer with the lower Tm base (A or T). Ideally, forward primers were 15–20 bp long (our average length was 19 bp) and had a melting temperature ranging from 59°C–62°C without the GC clamp (our average Tm was 50°C). Common reverse primers were designed no more than 20 base pairs downstream from the SNP and had an optimal length of 22–27 bp (our average length was 25 bp) with a melting temperature between 63°C and 70°C without the GC clamp (our average Tm was 57°C). PCRs were set up as follows in 15 μl volumes: 10 ng of genomic DNA; 0.2 μM each of the three primers, 1.8 U of Taq Gold, 10 mM Tris-HCl (pH 8), 40 mM KCl, 2 mM MgCl2, 50 μM each dATP, dCTP, and dGTP; 25 μM dTTP; 75 μM dUTP; 0.2× SYBR Green nucleic acid gel stain; 5% DMSO; and 2.5% glycerol. PCR and melting-curve analysis was preformed in Hard-Shell Thin-Wall 96-Well Microplates (Bio-Rad Laboratories, Hercules, CA) and sealed with Flat Cap Strips (Bio-Rad). PCR was performed on the DNA Tetrad Engine 2 (MJ Research). An initial incubation step at 95°C for 6 min was followed by 40 cycles of a three-step amplification process, which consists of 20 s at 95°C for denaturation, 30 s at 59°C (or optimal primer temperature) for annealing, and 30 s at 72°C for extension. Samples were then incubated for 10 min at 72°C for final extension. Melting-curve analysis was preformed on the Opticon continuous fluorescence detection system (MJ Research). Samples were first incubated at 55°C for 5 s. Fluorescence intensity was then detected with a melting curve from 60°C to 92°C. Readings were taken every 0.2°C and held for 1 s between reads. We selected 43 SNPs for genotyping by using the Tm-shift method. Of these, 28 SNPs gave reliable calls across a control set of DNA samples and were used for genotyping blood and tissue pairs.

Quantitative Real-Time PCR

Quantitative real-time PCR (qPCR) was performed for the assessment of copy-number variation at the *GLI3* locus in a patient (2020; Figure 1) for the confirmation of the chromosomal abnormality found by copy-number analysis of high-density SNP genotyping. qPCR was not conducted on other samples because of limitations on nonamplified genomic DNA. The assay was performed on the My iQ single-color real-time PCR detection system (Bio-Rad) in Thermo-fast 96-well semi-skirted plates (Abgene, Epsom, UK) with iQ SYBR Green Supermix (Bio-Rad). Reaction mixtures consisted of 10 ng of DNA in 6 μl or 10 μl of SYBR Green Supermix, and 4 μl of 2 μM primer pair. Primer sequences are as follows: 5′-GTTGCACAAAGGCCTACTCG-3′ and 5′-CGTTCTGTTTTGGTG TTTGG-3′ (directed against exon 12 of *GLI3*); and 5′- GCTTCAGT CAGCAAGACACG-3′ and 5′-TGTCCACTGTGCTTGTCACC-3′ (directed against exon 15 of *GLI3*). The assay was performed with DNA isolated from both blood and HH tissue samples, and reactions were run in quadruplicate with the following conditions: 95°C for 5 min and then 40 cycles (95°C for 20 s and 60°C for 20 s). Melting-curve analysis was performed with readings taken every 1°C from 60°C to 95°C, with a dwell time of 5 s. *β-actin*

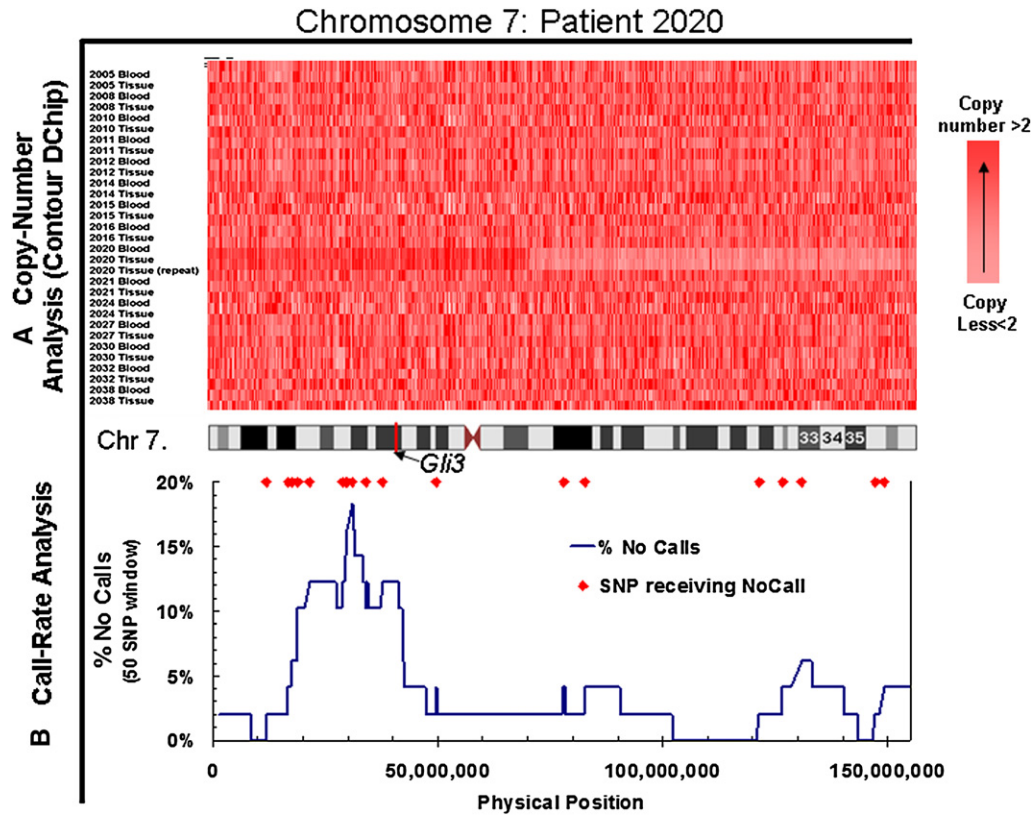

Figure 1. Chromosomal Abnormalities on 2020

Blood and tissue pairs were assayed on the Affymetrix 10K platform. Copy-number changes were calculated with the analysis software DChipSNP.[19] The amplification was later verified at the *GLI3* locus by qPCR.

(A) Copy-number analysis indicated that chromosome 7p had a copy number change to 2.5 copies for the tissue and not the blood, whereas all other samples showed no significant stretches of copy-number change. The assay was repeated for verification that the finding was not assay specific.

(B) The percent of SNPs receiving a No Call across a 50 SNP window is shown for sample 2020. It would be expected that the No Call rate would increase in a region containing an amplification because SNPs would not easily bin into AA, AB, and BB, as would be the case if the copy number were two or one. Within the 7p region is the *GLI3* gene, previously shown to harbor germline mutations causing Pallister Hall syndrome, which is highly associated with HH.

(*ACTB* [MIM 102630]) was used as the endogenous control, with the following primer pair: 5′-GGACTTCGAGCAAGAGATGG-3′ and 5′- AAGGAAGGCTGGAAGAGTGC-3′. Copy number was calculated with the $2^{-\Delta\Delta}C_T$ method as described.[18]

Results

Whole-Genome Screening for LOH and Altered Copy Number

To identify somatic chromosomal abnormalities specific to HH tissue, we genotyped each of 26 blood and HH tissue pairs on the Affymetrix 10K GeneChip SNP genotyping microarrays. By utilizing this platform, we could (1) identify stretches of LOH where SNPs were heterozygous in blood and homozygous in tissue and (2) assess for copy-number changes by analyzing probe-intensity data.

Quality Control for Affymetrix 10K Genotype Data

Genotype data underwent a two-stage strict quality-control filter so that accuracy could be ensured. Quality control was first employed at a sample level. Of the 26 paired blood and HH tissue samples, 21 samples passed a strict quality-control metric of having greater than 90% of all genotypes called for both blood and HH tissue samples. However, those samples not passing the 90% threshhold were also inspected by copy-number analysis in DChipSNP[19] and by preferential biases for SNPs that were not called. In this inspection, we were specifically assessing whether a large chromosomal abnormality was contributing to the low call rate. For those five samples, there was no evidence for chromosomal abnormalities contributing to the lower call rate. It is likely that these samples failed because of limited or poor DNA quality. Overall call rate for those samples passing the quality control metric was 93.2%. Quality-control filtering was also applied at the SNP level. The call rate for each SNP across blood samples was calculated, and SNPs with less than 95% call rate were removed from further analysis. After this two-stage filter, 7833 SNPs giving high-quality data remained.[20]

Analysis for Chromosomal Abnormalities

The paired blood and HH tissue samples of the 21 samples from above were examined for chromosomal abnormalities with DChipSNP. Rather than analyzing exclusively genotype data, DChipSNP uses probe-intensity data compared to a reference, or reference samples, to estimate copy number.[19] Previous studies and our own efforts have found that DChipSNP can effectively detect both deletions and amplifications covering multiple SNPs on Affymetrix arrays.[21] The exact lower limit is to our knowledge not known, and is likely dependent on coverage and SNP behavior.

For the 21 paired blood and HH tissue samples, only one sample exhibited strong evidence for a chromosomal abnormality, showing an amplification on chromosome 7p. Interestingly, inspection of the underlying copy-number estimates finds that the SNPs within the region generally average about 2.5 copies, with an estimate of 1.8 copies for the remainder of chromosome 7, and also on other chromosomes. Because copy-number analysis is not proven to be quantitatively accurate, we also inspected genotype data. If the region was amplified, we would also expect an increase in No Calls for SNPs within this region because SNPs would fall out of the three class (AA, AB, and BB) bins utilized by the MPAM (modified partitioning around medoids) Affymetrix GeneChip calling algorithm. In an amplified region, genotypes that are AAB, ABB, etc. would likely receive No Calls, because they would fall out of the genotype-calling silhouette.[22] Consistent with an amplification at 7p and shown in Figure 1, we find that there is a sharp increase in the percent of SNPs receiving a No Call within a 50 SNP sliding window, peaking at nearly 18%, whereas the genome-wide No Call rate is 6% ($p = 2 \times 10^{-10}$). These two analyses provide independent evidence for an amplification of 7p in HH tissue in this single case. To confirm the amplification specifically within the *GLI3* locus, we designed qPCR reactions for the 12th and 15th exons as described in the methods. Copy numbers of 3.97 and 4.23 for exons 12 and 15, respectively, were calculated with the 2-$^{\Delta\Delta}$CT method,[18] confirming the chromosomal abnormality by a separate method.

Genome-Wide Analysis for Loss of Heterozygosity

Because both whole-blood and HH tissue genotype data were available, we examined paired samples for LOH at a genome-wide level. A change of genotype from heterozygous in blood to homozygous in HH tissue constitutes an LOH event. Given the number of SNPs and samples genotyped, some LOH events are expected because of the number of markers genotyped. For the 21 paired samples across the 7833 SNPs, we observed a mean of 8.2 LOH events per paired sample (range 1–22 LOH events per paired sample). This number of LOH events is expected given the reported genotype error rate of the platform (~0.2%). Consequently, we made the additional requirement that two consecutive LOH events must occur at informative SNPs. The probability of two consecutive LOH events will be less than 1×10^{-5} for any one sample. Across all samples, we did not observe two consecutive LOH events within any paired set, establishing that large-scale LOH is not observed in paired blood and HH tissue samples. Considering the number of SNPs analyzed, an approximately 30% rate of SNP heterozygosity, and that LOH was only determined significant if it occurred in two consecutive LOH events (ignoring SNPs homozygous in blood), the resolution of this analysis is approximately 2 Mb (mean 1.81 Mb separation between two heterozygous SNPs). Thus, we conclude that large-scale somatic deletions do not contribute to the pathogenesis of HH lesions in sporadic, nonsyndromic cases.

GLI3 Resequencing in Blood and HH Tissue Pairs

Within the region exhibiting the chromosomal abnormality, we sequenced the exon and promoter regions for *GLI3* across 55 blood and HH tissue pairs with the objective of identifying germline and/or somatic mutations. Bidirectional sequence data were analyzed with Mutation Surveyor (SoftGenetics, State College, PA).

Based upon *GLI3* resequencing on genomic DNA isolated from peripheral blood, one case was identified with a germline mutation that had not been previously cataloged. This was a missense mutation in exon 15, leading to a serine to isoleucine substitution. This HH patient was a nondysmorphic, high-functioning adult female with refractory gelastic seizures as her only seizure type. Consequently, this mutation is more likely to be a benign polymorphism. It appears unlikely that germline mutations in *GLI3* lead to sporadic and otherwise nonsyndromic HH.

However, we did find evidence for loss of heterozygosity in the blood and HH tissue pairs, consistent with somatic mutations in HH tissue. Specifically, within 3 of the 55 (5%) sequenced blood and HH tissue pairs, LOH was observed at a resequenced SNP. Summarized as part of Figure 2, LOH was observed by direct resequencing on exon 7 of patient 2038, exon 15 of patient 2075, and exon 5 of patient 2030. In all cases, we repeated sequence reactions and used bidirectional sequence traces to confirm that the LOH event was accurate. The finding of LOH in 3/55 individuals is likely an underestimate because a heterozygote SNP (or other polymorphisms) was required to identify loss of one allele. Thus, given this additional evidence for LOH in *GLI3*, we selected a panel of 43 SNPs for custom genotyping by using the Tm-shift technique.

Additional Custom Genotyping of *GLI3*

Because of the limited capability of resequencing to identify LOH, we genotyped an additional set of SNPs across the *GLI3* gene. Sufficient unamplified genomic DNA was available for 26 of the 55 blood and HH tissue pairs. The same 26 pairs were utilized for the whole-genome microarray screening reported above. We selected SNPs with 40%–50% heterozygosity to provide approximate even coverage across *GLI3* by using HapMap resource.[23] We constructed and validated assays by following the

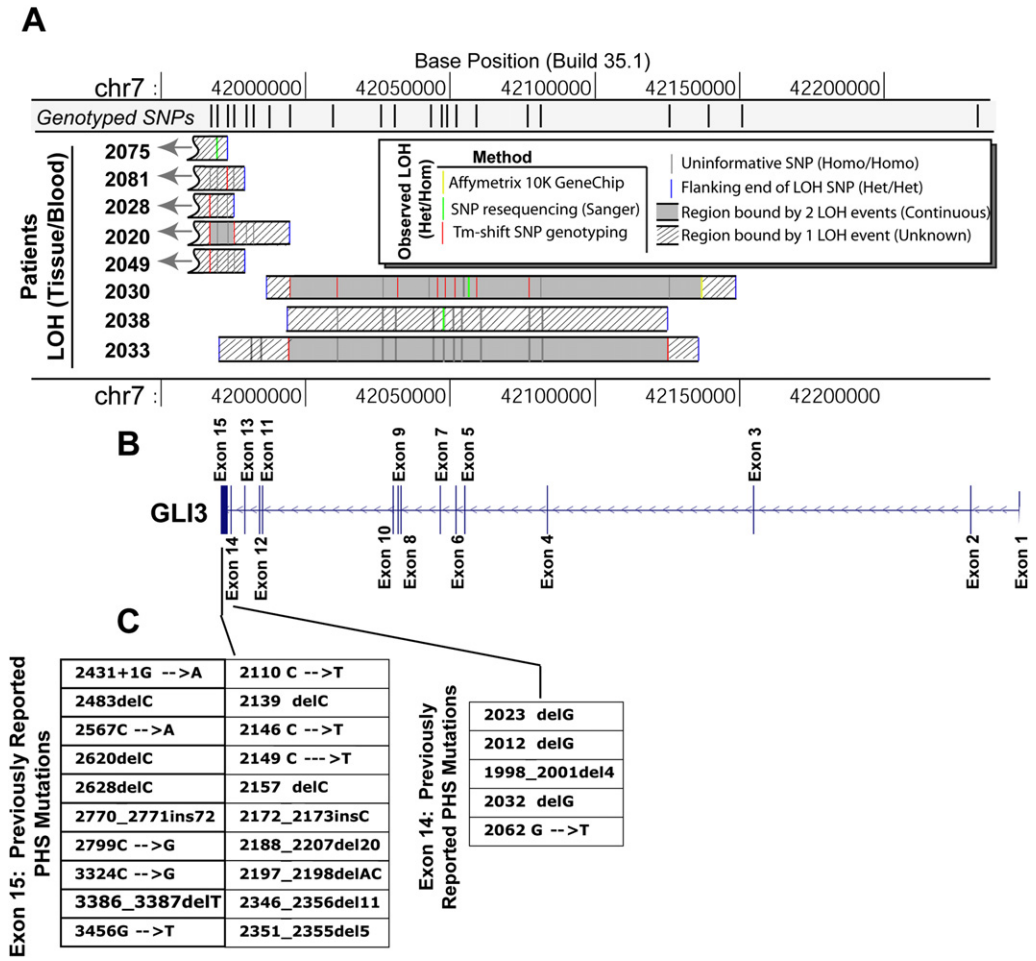

Figure 2. Observed Loss of Heterozygosity within *GLI3* Gene for HH Blood and Tissue Paired Samples

LOH was detected either by resequencing, genotyping on the Affymetrix platform, or custom SNP-genotyping with Tm-Shift assays. LOH events were defined as pairs in which the blood sample contained a heterozygous polymorphism (e.g., a heterozygote SNP) and the tissue sample was homozygous. SNPs that were genotyped homozygous in blood were uninformative (shown as gray bars). Samples where a heterozygote was observed in both the tissue and blood samples indicate the absence of LOH.

(A) A total of eight samples contained LOH events observed by either genotype data from the Affymetrix 10K GeneChip mapping array (yellow bar), sequencing of a heterozygous SNP within exons (green bar), or SNP genotyping (red bar). Blue bars indicate the nearest flanking SNP to an LOH even (green, yellow, and red bars) where LOH was definitively not observed. Uninformative SNPs that were not within a region of LOH or SNPs that were heterozygous in blood and tissue but did not neighbor an LOH event are not shown, for clarity.

(B) Schematic of *GLI3* gene aligned to above LOH graphs.

(C) Mutations within the *GLI3* gene have previously been found to lead to Pallister-Hall Syndrome (PHS).

Tm-shift method as described by Wang[17] for 28 SNPs across the *GLI3* gene. Assays were validated by the demonstration of distinct calls for all possible genotype calls across a control panel of HapMap samples. Genotype calling was manually accomplished by the inspection of all samples and the visual identification of three classes of Tm-shift peaks. Any genotyped SNP was informative only if the blood sample gave a heterozygote call. Of the 26 HH patients, consistent and reliable calls could be obtained for 24.

LOH events within *GLI3* were observed in 6 of 24 blood and HH tissue pairs (25%) by custom SNP genotyping (Figure 2). The endpoint of a putative LOH region was determined by the identification of flanking SNPs that were heterozygous in both blood and HH tissue. For example, for patient 2030, multiple LOH events are surrounded by two SNPs that were heterozygous in blood and tissue. Flanking SNPs were not identified for some samples whose most proximal or distal SNP was either homozygous in both blood and tissue or an LOH event.

Considering all three genotyping techniques together, one patient [patient 2030, (Figure 2)] demonstrated a total of nine LOH events in the *GLI3* region by whole-genome microarray screening, *GLI3* resequencing, and fine mapping of *GLI3* by SNP genotyping. Patients 2033 and 2020 (Figure 2) exhibited two LOH events each. All other patients had one observed LOH event identified. SNPs exhibiting LOH and bounding SNPs for which both blood and

Table 2. SNPs Exhibiting Loss of Heterozygosity from Tissue to Blood

Patient	LOH Event	Flanking SNPs (No Observed LOH)
2075	257307GT→GG[Seq]	rs2051935, rs7782675
2081	rs4724083	n/a, rs10263647
2028	rs2051935	rs1181740[A], rs10263647
2020	rs2051935, rs7776918	rs1181740[A], rs3898405
2049	rs2051935	rs217034, rs99487
2030	rs699487, rs10282353, rs699494, rs846312[A], rs846274, rs846329, rs699493, rs846322	rs10263647, rs6463092
2038	183130CT→CC[Seq]	rs7782675, rs1367590
2033	rs9648515, rs99497	rs10263647, rs846312[A]

Superscript "A" indicates found by Affymetrix, and superscript "Seq" indicates found by sequencing; all others were found by SNP genotyping.

tissue showed heterozygosity at the same base are listed in Table 2.

Discussion

Although uncommon, hypothalamic hamartomas are an important model of human epilepsy.[8,24] It is the single best model for subcortical epilepsy in humans. Utilizing surgically resected HH tissue, it is also an excellent model for the study of basic molecular and cellular mechanisms that result in intrinsic epileptogenesis.[25,26]

PHS is the most common dysmorphic syndrome associated with HH.[10] HH is a hallmark, if not a universal feature of PHS.[27] PHS is associated with mutations within *GLI3*, a zinc-finger transcription factor within the sonic hedgehog intracellular signaling pathway.[14] *GLI3* is located at 7p13 and consists of 15 exons, with the majority of the coding sequence found in the last two exons.[28] A genotype-phenotype relationship has been described for *GLI3*, which is known to function normally as either an activator or repressor of gene expression in response to sonic hedgehog signaling.[27,29] Specifically, Greig cephalopolysyndactaly syndrome (GCPS [MIM 175700]), a dysmorphic syndrome with polydactyly and craniofacial anomalies but without HH) results from loss-of-function mutations in specific regions of the gene that result in haploinsufficiency of the gene.[29] Alternatively, PHS patients have mutations in the middle third of the coding region of the gene that result in a protein that fails to respond to normal regulatory control.[29] Consequently, in PHS, the protein functions in a constitutively active manner as a repressor of those genes under its downstream control.[30]

The genetic mechanism(s) that result in HH in sporadic, nonsyndromic cases is unknown. We first performed a genome-wide screen with SNP microarrays, looking for LOH and/or copy-number changes as evidence of a somatic (tumor-only) mutation. LOH in HH tissue (versus blood) typically implies a deletion of one of the two heterozygous alleles at a known SNP locus. The presence of LOH at contiguous informative SNPs implies a deletion event, although other complex chromosomal abnormalities could also lead to the observation of LOH at a given SNP. In our initial genome-wide analysis for LOH, we did not observe consecutive LOH events in any of the samples. Occasional sporadic LOH events at a given SNP were observed, though entirely consistent with the Affymetrix error rate. However, analysis of genome-wide SNP microarray copy-number data did demonstrate one large chromosomal abnormality in HH tissue, consisting of an amplification of the short arm of chromosome 7 [see (Figure 1)]. Because this was observed in only a single case, the significance of this finding for other sporadic, nonsyndromic HH cases is limited, though it warrants further investigation. The region spanned several million base pairs, which is too large to enable a candidate gene approach (although it is notable that this stretch of DNA does include *GLI3*).

On the basis of n this large-scale chromosomal abnormality limited to chromosome 7p, further study focused on the possibility of acquiring somatic mutations within *GLI3* in HH tissue. By resequencing and custom SNP genotyping of the *GLI3* locus, we identified LOH events within eight blood and HH tissue pairs from a total study group of 55 HH cases (15%). Utilizing *GLI3* resequencing, we identified possible somatic mutations in 3 of 55 cases (5%), whereas SNP genotyping determined possible somatic mutations in 6 of 24 cases (25%). Furthermore, genotyping on the Affymetrix 10K platform found one LOH event in 24 cases within *GLI3*. One case (2030) was identified by all three methods within the *GLI3* gene. Noteworthy, LOH was restricted to the *GLI3* gene and was not prevalent in a genome-wide scan by the Affymetrix 10K for this individual. Taken together, these results find that somatic chromosomal abnormalities occur at the *GLI3* locus within HH tissue and help shed light onto potential mechanisms for HH pathogenesis. LOH results from the acquisitions of somatic mutations at one or both of the copies of *GLI3,* resulting in an uneven balance of the two alleles. This finding is consistent with the finding that PHS is known to result from haploinsufficiency of *GLI3*, but future research is needed to determine the mechanism by which somatic mutations in *GLI3* contribute to the development of HH.[14]

However, as noted above, a rather specific genotype-phenotype model has been proposed for the *GLI3* gene, with Pallister-Hall syndrome (and its association with HH) occurring secondary to loss-of-function mutations with the middle third of the coding region (open reading frame [ORF] nucleotides [nt] 1998–3481 found in exons 13, 14, and 15), resulting in the loss of a regulatory domain.[27,29] The somatic LOH events found in sporadic HH were mostly found to span exons 12, 13, 14, and 15. The technology used in this study and the expectation that chromosomal abnormalities leading to LOH would span large regions (>1 KB) make it difficult to distinguish breakpoints within these exons. This is particularly the case for exons

14 and 15, wherein most of the coding sequence lies and where previous PHS mutations are described. Rather, it can be said there appeared to be a preferential bias for detecting LOH in exons 14 and 15, previously linked to PHS. We did not observe any LOH events in the exons 1 through 3. Although there does appear to be a relationship between sporadic HH lesions and somatic mutations in *GLI3* in at least a subset of patents, it is also apparent that there is a high degree of variability in these mutations because no single patient had the same somatic mutation of the eight cases identified in this population. This is consistent with other solitary lesions, such as the large number of different somatic mutations that can occur in the *VHL* tumor suppressor gene (MIM 608537) in sporadic clear cell renal carcinoma.[31] Further refinements in genotyping technology might allow for the identification of somatic mutations of *GLI3* in a higher percentage of cases.

Nevertheless, these results would also suggest that most sporadic HH cases are *not* due to a somatic mutation of *GLI3* and that another mechanism, or multiple other mechanisms, including the possibility of somatic mutation in other genes or regions, is responsible. This is also consistent with other disease models. Sporadic pheochromocytoma, for example, has been associated with somatic mutations in *VHL*, *RET* (MIM 164761), or *SBHD* genes, each in a relatively small proportion of cases.[32–34]

One other candidate gene has been implicated in HH pathogenesis in patients with HH associated with other developmental anomalies. Loss-of-function mutations in *SOX2* (MIM 184429), a transcription factor in the SOX family that makes use of an HMG box DNA-binding domain, has been associated with a spectrum of abnormalities, including developmental eye defects (anophthalmia and microphthalmia), anterior pituitary hypoplasia, and other midline cerebral defects. A recent report describes HH lesions (without an associated history of epilepsy) in two of eight cases (25%) with germline mutations in *SOX2*.[35] It is unknown whether somatic mutations in *SOX2* are associated with HH in sporadic, nonsyndromic cases. An additional susceptibility locus for HH has also been reported, on the basis of the observation of a small duplication or deletion at 6p25.1–25.3 in a patient with HH, refractory epilepsy, and subtle dysmorphic features.[36] This affected region includes *FOXC1* (MIM 601090), a transcription factor in the forkhead family, as a possible candidate gene for HH pathogenesis.

The findings reported here provide evidence that somatic mutation in *GLI3* is a potential etiology for the occurrence of HH associated with epilepsy in sporadic, nonsyndromic patients. Depending upon the specific genotyping technology used to compare genomic DNA derived from peripheral blood and HH tissue, we have observed LOH in the region of *GLI3* in 5% to 25% of patients undergoing surgical resection of HH for refractory epilepsy. Conversely, a genome-wide screen for LOH demonstrates that large-scale somatic deletions are not associated with sporadic HH.

Acknowledgments

D.W.C. and A.I. were funded by a Stardust Foundation grant. J.F.K. was funded by a grant from the Barrow Neurological Foundation.

Received: July 31, 2007
Revised: October 4, 2007
Accepted: October 15, 2007
Published online: January 31, 2008

Web Resources

The URL for data presented herein is as follows:

Online Mendelian Inheritance in Man (OMIM), http://www.ncbi.nlm.nih.gov/Omim/

References

1. Brandberg, G., Raininko, R., and Eeg-Olofsson, O. (2004). Hypothalamic hamartoma with gelastic seizures in Swedish children and adolescents. Eur. J. Paediatr. Neurol. *6*, 35–44.
2. Berkovic, S.F., Andermann, F., Melanson, D., Ethier, R.E., Feindel, W., and Gloor, P. (1998). Hypothalamic hamartomas and ictal laughter: Evolution of a characteristic epileptic syndrome and diagnostic value of magnetic resonance imaging. Ann. Neurol. *23*, 429–439.
3. Valdueza, J.M., Cristante, L., Dammann, O., Bentele, K., Vortmeyer, A., Saeger, W., Padberg, B., Freitag, J., and Herrmann, H.-D. (1994). Hypothalamic hamartomas: With special reference to gelastic epilepsy and surgery. Neurosurgery *34*, 949–958.
4. Arita, K., Ikawa, F., Kurisu, K., Sumida, M., Harada, K., Uozumi, T., Monden, S., Yoshida, J., and Nishi, Y. (1999). The relationship between magnetic resonance imaging findings and clinical manifestations of hypothalamic hamartoma. J. Neurosurg. *91*, 212–220.
5. Jung, H., Probst, E.N., Hauffa, B.P., Partsch, C.J., and Dammann, O. (2003). Association of morphological characteristics with precocious puberty and/or gelastic seizures in hypothalamic hamartoma. J. Clin. Endocrinol. Metab. *88*, 4590–4595.
6. Deonna, T., and Ziegler, A.-L. (2000). Hypothalamic hamartoma, precocious puberty and gelastic seizures: a special model of "epileptic" developmental disorder. Epileptic Disord. *2*, 33–37.
7. Arzimanoglou, A.A., Hirsch, E., and Aicardi, J. (2003). Hypothalamic hamartoma and epilepsy in children:illustrative cases of possible evolutions. Epileptic Disord. *5*, 187–199.
8. Kerrigan, J.F., Ng, Y.-t., Chung, S.S., and Rekate, H.R. (2005). The hypothalamic hamartoma: A model of subcortical epileptogenesis and encephalopathy. Semin. Pediatr. Neurol. *12*, 119–131.
9. Ng, Y.-t., Rekate, H.L., Prenger, E.C., Chung, S.S., Feiz-Erfan, I., Wang, N.C., Varland, M.R., and Kerrigan, J.F. (2006). Transcallosal resection of hypothalamic hamartoma for intractable epilepsy. Epilepsia *47*, 1192–1202.
10. Biesecker, L.G. (2003). Heritable syndromes with hypothalamic hamartoma and seizures: Using rare syndromes to understand more common disorders. Epileptic Disord. *5*, 235–238.
11. Biesecker, L.G., Abbott, M., Allen, J., Clericuzio, C., Feuillan, P., Graham, J.M. Jr., Hall, J., Kang, S., Olney, A.H., Lefton, D., et al.

(1996). Report from the workshop on Pallister-Hall syndrome and related phenotypes. Am. J. Med. Genet. *65*, 76–81.
12. Kletter, G.B., and Biesecker, L.G. (1992). Male-to-male transmission of the Pallister-Hall syndrome. Am. J. Hum. Genet. suppl. *51*, A100.
13. Kang, S., Allen, J., Graham, J.M. Jr., Grebe, T., Clericuzio, C., Patronas, N., Ondry, F., Green, E., Schaffer, A., Abbott, M., et al. (1997). Linkage mapping and phenotypic analysis of autosomal dominant Pallister-Hall syndrome. J. Med. Genet. *34*, 441–446.
14. Kang, S., Graham, J.M. Jr., Olney, A.H., and Biesecker, L.G. (1997). *GLI3* frameshift mutations cause autosomal dominant Pallister-Hall syndrome. Nat. Genet. *15*, 266–268.
15. Delalande, O., and Fohlen, M. (2003). Disconnecting surgical treatment of hypothalamic hamartoma in children and adults with refractory epilepsy and proposal of a new classification. Neurol. Med. Chir. (Tokyo) *43*, 61–68.
16. Kennedy, G.C., Matsuzaki, H., Dong, S., Liu, W.M., Huang, J., Liu, G., Su, X., Cao, M., Chen, W., Zhang, J., et al. (2003). Large-scale genotyping of complex DNA. Nat. Biotechnol. *21*, 1233–1237.
17. Wang, J., Chuang, K., Ahluwalia, M., Patel, S., Umblas, N., Mirel, D., Higuchi, R., and Germer, S. (2005). High-throughput SNP genotyping by single-tube PCR with Tm-shift primers. Biotechniques *39*, 885–893.
18. Livak, K.J., and Schmittgen, T.D. (2001). Analysis of relative gene expression data using real-time quantitative PCR and the $2^{-\Delta\Delta C}{}_{T}$ method. Methods *25*, 402–408.
19. Lin, M., Wei, L.J., Sellers, W.R., Lieberfarb, M., Wong, W.H., and Li, C. (2004). dChipSNP: Significance curve and clustering of SNP-array-based loss-of-heterozygosity data. Bioinformatics *20*, 1233–1240.
20. Huentelman, M.J., Craig, D.W., Shieh, A.D., Corneveaux, J.J., Hu-Lince, D., Pearson, J.V., and Stephan, D.A. (2005). SNiPer: Improved SNP genotype calling for Affymetrix 10K GeneChip microarray data. BMC Genomics *6*, 149.
21. Leykin, I., Hao, K., Cheng, J., Meyer, N., Pollak, M.R., Smith, R.J., Wong, W.H., Rosenow, C., and Li, C. (2005). Comparative linkage analysis and visualization of high-density oligonucleotide SNP array data. BMC Genet. *6*, 7.
22. Di, X., Matsuzaki, H., Webster, T.A., Hubbell, E., Liu, G., Dong, S., Bartell, D., Huang, J., Chiles, R., Yang, G., et al. (2005). Dynamic model based algorithms for screening and genotyping over 100 K SNPs on oligonucleotide microarrays. Bioinformatics *21*, 1958–1963.
23. Thorisson, G.A., Smith, A.V., Krishnan, L., and Stein, L.D. (2005). The International HapMap Project Web site. Genome Res. *15*, 1592–1593.
24. Berkovic, S.F., Arzimanoglou, A., Kuzniecky, R., Harvey, A.S., Palmini, A., and Andermann, F. (2003). Hypothalamic hamartoma and seizures: A treatable epileptic encephalopathy. Epilepsia *44*, 969–973.
25. Wu, J., Xu, L., Kim, D.Y., Rho, J.M., St. John, P.A., Lue, L.-F., Coons, S., Ellsworth, K., Nowak, L., Johnson, E., et al. (2005). Electrophysiological properties of human hypothalamic hamartomas. Ann. Neurol. *58*, 371–382.
26. Fenoglio, K.A., Rho, J.M., Wu, J., Kim, D.Y., Simeone, T.A., Coons, S.W., Rekate, H.L., and Kerrigan, J.F. (2007). Hypothalamic hamartoma: Basic mechanisms of intrinsic epileptogenesis. Semin. Pediatr. Neurol. *14*, 51–59.
27. Biesecker, L.G. (2006). What you can learn from one gene: *GLI3*. J. Med. Genet. *43*, 465–469.
28. Kang, S., Rosenberg, M., Ko, V.D., and Biesecker, L.G. (1997). Gene structure and allelic expression assay of the human GLI3 gene. Hum. Genet. *101*, 154–157.
29. Johnston, J.J., Olivos-Glander, I., Killoran, C., Elson, E., Turner, J.T., Peters, K.F., Abbott, M.H., Aughton, D.J., Aylsworth, A.S., Bamshad, M.J., et al. (2005). Molecular and clinical analyses of Greig cephalopolysyndactyly and Pallister-Hall syndromes: Robust phenotype prediction from the type and position of *GLI3* mutations. Am. J. Hum. Genet. *76*, 609–622.
30. Shin, S.H., Kogerman, P., Lindstrom, E., Toftgard, R., and Biesecker, L.G. (1999). *GLI3* mutations in human disorders mimic Drosophila cubitus interruptus protein functions and localizations. Proc. Natl. Acad. Sci. USA *96*, 2880–2884.
31. Gnarra, J.R., Tory, K., Weng, Y., Schmidt, L., Wei, M.H., Li, H., Latif, F., Liu, S., Chen, F., Duh, F.-M., et al. (1994). Mutations of the VHL tumour supressor gene in renal carcinoma. Nat. Genet. *7*, 85–90.
32. Eng, C., Smith, D.P., Mulligan, L.M., Nagal, M.A., Healey, C.S., Ponder, M.A., Gardner, E., Scheumann, G.F.W., Jackson, C.E., Tunnacliffe, A., et al. (1994). Point mutation within the tyrosine kinase domain of the RET proto-oncogene in multiple endocrine neoplasia type 2B and related sporadic tumours. Hum. Mol. Genet. *3*, 237–241.
33. Hofstra, R.M.W., Stelwagen, T., Stulp, R.P., De Jong, D., Hulsbeek, M., Kamsteeg, E.J., Van Den Berg, A., Landsvater, R.M., Vermey, A., Molenaar, W.M., et al. (1996). Extensive mutation scanning of RET in sporadic medullary thyroid carcinoma and of RET and VHL in sporadic pheochromocytoma reveals involvement of these genes in only a minority of cases. J. Clin. Endocrinol. Metab. *81*, 2881–2884.
34. Maher, E.R., and Eng, C. (2002). The pressure rises: Update on the genetics of pheochromocytoma. Hum. Mol. Genet. *11*, 2347–2354.
35. Kelberman, D., Rizzoti, K., Avilion, A., Bitner-Glindzicz, M., Cianfarani, S., Collins, J., Chong, W.K., Kirk, J.M.W., Achermann, J.C., Ross, R., et al. (2006). Mutations within *Sox2/SOX2* are associated with abnormalities in the hypothalamo-pituitary-gonadal axis in mice and humans. J. Clin. Invest. *116*, 2442–2455.
36. Kerrigan, J.F., Kruer, M.C., Corneveaux, J., Panganiban, C.B., Itty, A., Reiman, D., Ng, Y.-t., Stephan, D.A., and Craig, D.W. (2007). Chromosomal abnormality at 6p25.1–25.3 identifies a susceptibility locus for hypothalamic hamartoma associated with epilepsy. Epilepsy Res. *75*, 70–73.